Wind tunnel calibration of cup anemometers

Ole Frost Hansen, WindSensor ApS
Svend Ole Hansen, Svend Ole Hansen ApS
Leif Kristensen

Wind Tunnel Calibration of Cup Anemometers

Ole Frost Hansen, Svend Ole Hansen and Leif Kristensen

AUTHORS QUALIFICATIONS

Ole Frost Hansen, B.Sc. in Electronic Engineering
Svend Ole Hansen, M.Sc. in Civil and Structural Engineering, Ph.d. in Wind Engineering
Leif Kristensen, M.Sc. in Nuclear Physics, Dr. Techn. in Metrology

AUTHORS AFFILIATIONS

Director of WindSensor ApS, Søkrogen 9, DK-4000 Roskilde, Denmark

E-mail: ole.frost@windsensor.dk, Phone +45 46 38 36 28

Director of Svend Ole Hansen ApS, Sct. Jørgens Allé 5, DK-1615 Copenhagen, Denmark

E-mail: soh@sohansen.dk, Phone: +45 33 25 38 38, Fax: +45 33 25 38 39

Leif Kristensen, E-mail: leif.kristensen@net.telenor.dk

KEYWORDS

Wind tunnels, calibration of cup anemometers, tilt angular response and rotor torque characteristics of cup anemometers, Measnet, IEC 61400-12-1.

CONTENTS

Number of words in main text: approx. 6.800.
2 tables.
14 figures.

ABSTRACT

The paper describes wind tunnel calibrations of cup anemometers and classification of cup anemometers based on wind tunnel measurements of their tilt angular response and rotor torque characteristics. The results are used for power-performance and wind-resource estimates, and all measurements applied follow the procedures specified in IEC 61400-12-1 and are carried out in wind tunnels being accredited and Measnet approved.

Cup anemometer aerodynamics and wind tunnel aerodynamics are considered and used to evaluate the uncertainties involved in cup anemometer calibrations. The IEC procedure for cup anemometer calibrations specifies flow requirements of the empty working section, e.g. requirements concerning flow homogeneity and upper limit of flow turbulence, and tunnel size in form of maximum blockage ratios. The paper documents that deviation between full-scale and model-scale air turbulence and the interference effects between tunnel boundaries and rotating rotors of cup anemometers including their mounting systems may introduce a significant bias on the calibration results. This, however, is not taken into consideration by the specifications of the IEC procedure.

The importance of distance from cup anemometer rotor to tunnel boundaries is illustrated for both open and closed tunnels. It is shown that a certain minimum distance from rotor to tunnel boundary is crucial for avoiding significant contributions from these interference effects. If this distance is too small the tunnel boundary may be sucked towards the rotor in open tunnels or a friction force may be generated in closed tunnels. The suction towards the rotor in open tunnels may lead to accelerated flow in the central part of the cross section, and thereby increased rotation rate of the rotor. The friction force in closed tunnels will decrease the rotation rate of the rotor. Thus, interference effects as the ones described above will systematically bias the calibration results obtained significantly for small wind tunnels with a short distance from rotor to tunnel boundaries.

The present IEC procedure is based on a number of assumptions, which may lead to deviating calibration results. We recommend that the ongoing revision of the IEC procedure takes the new findings into consideration and that the effects shall be quantified by carrying out reference calibrations in very large wind tunnels with negligible contributions from blockage and tunnel boundary interference effects. In this way the updated procedure will reduce calibration uncertainties to a minimum and thereby minimize the uncertainties inherent in wind resources estimated for a specific site.

NOMENCLATURE

a	shape factor used to determine influence of blockage
A	slope of calibration equation
A_c	cross-sectional area of a single cup
b	blockage ratio
B	offset of calibration equation
c_f	force coefficient cup anemometer including its mounting system
C	force coefficient of single cup
d	characteristic dimension of rotor
h	height of building
I_v	longitudinal turbulence intensity
KC	Keulegan-Carpenter number
M	torque
n	frequency
r	distance from the anemometer hub to the center of the cup
t	time
v	incoming undisturbed wind velocity
v_b	changed wind velocity due to blockage
v_{rel}	relative wind velocity
v_{tilt}	angular velocity in a sweep for determining the tilt angular response
z_0	roughness length
α	angle of relative wind velocity
ρ	density of air
θ	angular position of cup
ω	angular velocity
ω_{eq}	equilibrium angular velocity

1. INTRODUCTION

The paper discusses wind tunnel calibration of cup anemometers and wind tunnel measurements used in the classification of cup anemometers.

Cup anemometer calibration results, and the tilt angular responses and rotor torque characteristics of cup anemometers measured in wind tunnels are outlined. The importance of distance from cup anemometer rotor to tunnel boundaries is illustrated. The main similarities and non-similarities between open and closed tunnels are discussed.

Methods for classification of cup anemometers were developed in the European research project Accuwind, see Dahlberg, Pedersen and Busche 2006, and the methods were subsequently implemented in the IEC 61400-12-1 standard on power performance measurements. The Accuwind results have been based on measurements carried out in relatively small wind tunnels, and the tilt angular response measurements were based on sweeps with a rate of approx. 2 degree per second. The paper shows that the limited tunnel heights and the sweep rate used in the Accuwind project will give systematic bias of the tilt angular responses determined in Accuwind.

The IEC procedures used are described and a number of improvements are suggested for revisions of the IEC standard. It is recommended that the new findings of the present paper are taken into account in the ongoing revision of the IEC standard.

The paper recommends procedures used to reduce the inherent calibration uncertainties in the present Measnet approved wind tunnels.

2. CUP ANEMOMETER AERODYNAMICS IN HORIZONTAL FLOW

The torque on a cup anemometer rotor is governed by wind forces on each individual cup of the rotor. These forces may be derived from the relative wind velocities experienced and the force coefficients as function of relative wind direction. The mathematical model is presented in section 2.1, and section 2.2 and 2.3 discuss the influence of air turbulence and Keulegan-Carpenter number KC, respectively.

2.1 Mathematical model

The mathematical model presented below is used in the rotor torque measurements described in section 6.2. It is assumed that the wind-induced torque on a single cup is not influenced significantly by flow distortion generated by the other two cups of the rotor.

The instantaneous torque on a cup anemometer is dependent on angular position θ, angular velocity ω and the incoming wind speed v. Even for equilibrium angular velocity ω_{eq} corresponding to v, the torque, and subsequently the angular velocity and position, fluctuate through each revolution. For the ith cup the torque M_i is calculated by

$$M_i(\theta,\omega,v) = \frac{1}{2}\rho v_{rel}^2(\theta,\omega,v)\, C(\alpha)\, A\, r \qquad (1)$$

in which $\alpha(\theta,\omega,v)$ is the angle of the relative wind velocity v_{rel} defined in figure 1. The torque is dependent on the angular position, angular velocity and incoming wind velocity

through the force coefficient $C(\alpha)$ and the instantaneous relative velocity $v_{rel}(\theta, \omega, v)$ squared, see figure 1. A is the cross-sectional area of a single cup, ρ is the density of air and r is the distance from the anemometer hub to the center of the cup.

A mathematical model based on averages over a revolution is established. The equation above is simplified and integrated with respect to θ and averaged for a complete revolution, thereby forming the following differential equation in ω:

$$I\frac{d\omega}{dt} = M_A + M_F \tag{2}$$

in which I is the mass moment of inertia of the rotor, M_A is the aerodynamic torque determined using equation (1), and M_F is the torque introduced by bearing friction.

The solution describes the angular response of the anemometer off its rotational equilibrium and implicitly determines the torque characteristics of the anemometer. The force coefficients are determined by wind tunnel tests.

The wind load on a single cup has been measured as function of wind direction for different turbulence characteristics, see figure 2 below. The influence of turbulence may hereby be determined using the mathematical model described above for the torque on a rotating rotor.

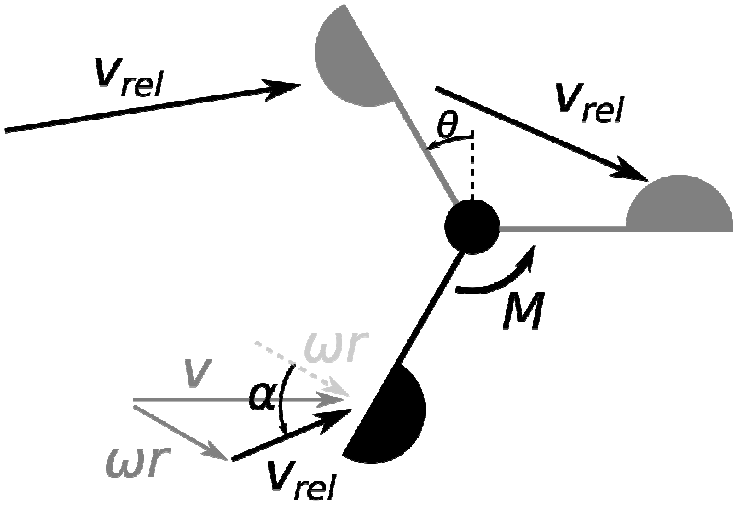

Figure 1. The figure shows the incoming wind vector v, the cup velocity ωr and the resulting relative wind velocities v_{rel} for a rotating rotor.

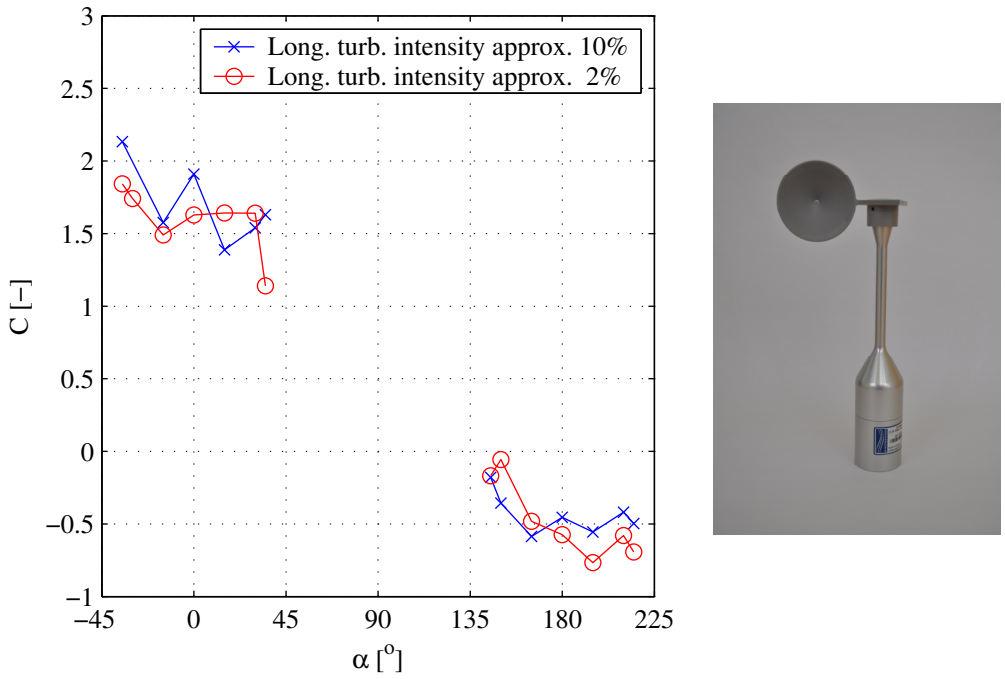

Figure 2. Measured force coefficients for a single WindSensor cup in a wind tunnel at two levels of longitudinal turbulence intensity. The angle on the x-axis and the force coefficient on the y-axis are defined in figure 1 and equation (1), respectively.

As shown in figure 2 the force coefficient may depend on the turbulence in the wind tunnel. This indicates that cup anemometer calibration results will also depend on the turbulence in the wind tunnel. In order to obtain accurate calibrations for full-scale situations with turbulence, especially the small scale turbulence and turbulence with larger length scales of the order of the rotor diameter, may be crucial to simulate in the wind tunnel, and this is not covered by the IEC specifications. The turbulence with length scales significantly larger than the rotor diameter and the distance constant of the cup anemometer corresponds to a slowly varying mean wind velocity, which is considered not to be crucial to simulate in the calibration itself. The influence of these larger turbulent length scales in form of overspeeding may be analyzed using the procedures described by Kristensen and Hansen 2012.

The dependence on turbulence described above shows that the present IEC target of low turbulence may lead to calibration results that are not representative for full-scale conditions in normal turbulent flows. A more accurate representation of full-scale turbulence, especially the small scale turbulence variations, will minimize potential calibration bias induced by mismatched turbulence conditions.

2.2 Wind-tunnel simulation of turbulence – a proposal

The importance of turbulence in the incoming wind was originally recognized in the 50'ties by Martin Jensen, see Jensen and Franck 1965. Martin Jensen measured the mean pressure coefficient at a point on a building roof for different turbulence characteristics, see figure 3. He showed that the mean pressure coefficient C_p, defined as the mean pressure p normalized by the mean velocity pressure q of the incoming wind, $C_p = p/q$, depends on

the dimensionless parameter of h/z_0 in which h is the height of the building and z_0 is the roughness length of the upstream terrain.

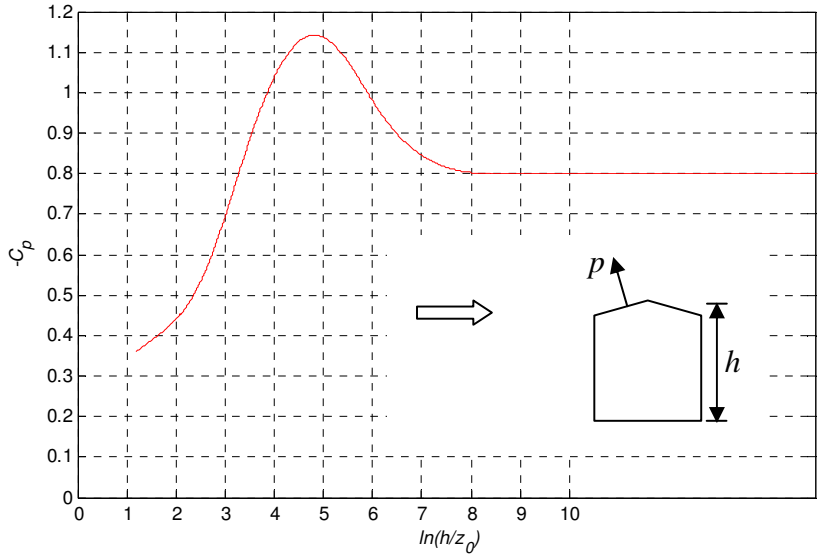

Figure 3. Pressure coefficient as function of turbulence, from (Jensen and Franck 1965). The abscissa is the natural logarithm of the Jensen number defined as the ratio between the height, h, of the house and the roughness length, z_0. The ordinate is the pressure coefficient for the suction at the centre of the windward roof surface (point p).

The results described above were the background for introducing the Jensen number Je defined as:

$$Je = \frac{h}{z_0} \tag{3}$$

which today is a basic similarity parameter considered in wind tunnel testing in turbulent flows, see Dyrbye and Hansen 1997.

The longitudinal turbulence intensity I_v at height h is often approximated by:

$$I_v = \frac{1}{\ln(h/z_0)} \tag{4}$$

indicating that the numbers on the x-axis of figure 3 are equal to $1/I_v$. A turbulence intensity of approx. 20% at building height is seen to give the largest mean suction in the roof point considered.

Thus, the influence of turbulence on the mean force coefficient shown in figure 2 is not surprising considering the results presented by Martin Jensen in 1965, see Jensen and Franck 1965. A simulation based on an accurate representation of small scale turbulence may be crucial for avoiding deviations in the calibrations carried out. This procedure is described in detail by Dyrbye and Hansen 1997 and here converted to possible wind tunnel air flow requirements for calibrations of cup anemometers, see figure 4 below.

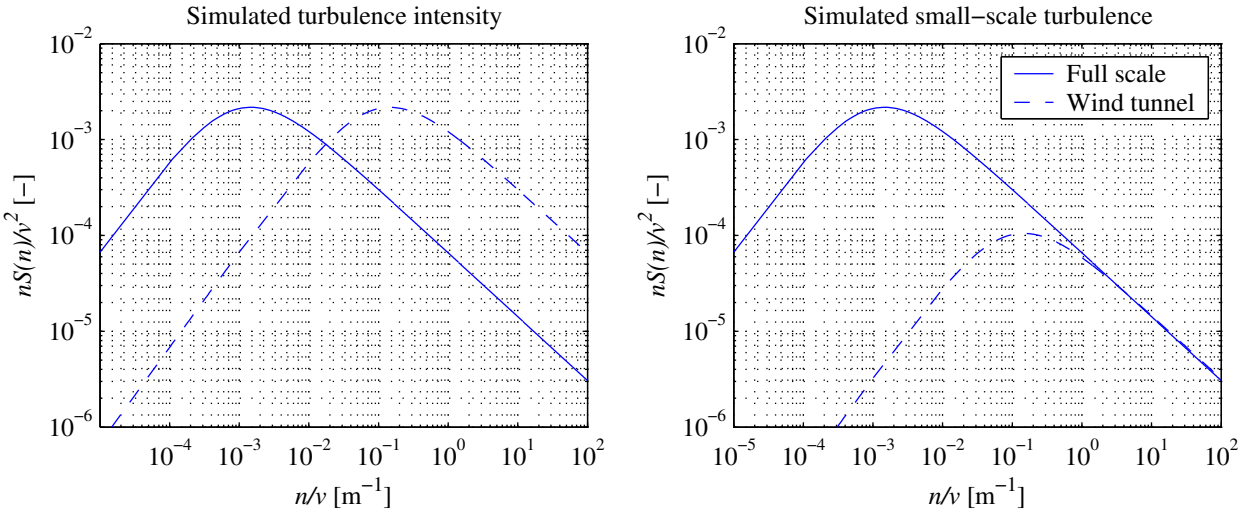

Figure 4. The left-hand figure shows a wind tunnel simulation based on a correct representation of the turbulence intensity assumed to be 10%. The right-hand figure shows a wind tunnel simulation with reduced turbulence intensity, but a correct representation of the small-scale turbulence. The turbulence intensity in the right-hand figure is approx. 2%.

The wind tunnel simulation illustrated in the right-hand figure 4 gives a correct representation of small-scale turbulence facilitating that the basic scaling of wind forces acting on the cups will have negligible bias. Thus, the calibration equation used to transform frequency to mean wind velocity will also be without any significant bias. It is not possible on the present basis to quantify accurately the influence of small-scale turbulence.

Overspeeding of cup anemometers have been analyzed in several papers and research reports, see e.g. Kristensen and Hansen 2012, Kristensen 1998 and Kristensen 1992. According to Kristensen 1992 a sudden increase of the wind speed gives a torque on the rotor which is numerically larger than a sudden decrease of the same magnitude. Since the rotation rate is not in equilibrium with the turbulent wind, which constantly has many small and fast changes up and down, the rotor will on average tend to run too fast with respect to the mean wind and thus give a positive bias.

Overspeeding in wind tunnels has been analyzed by Kristensen, Hansen and Hansen 2012. Inserting a turbulence intensity of 1-2% in the equation derived, see the right-hand figure 4, gives a bias of the order of 0.01% to 0.05% indicating that overspeeding is negligible in wind tunnel calibrations at low turbulence intensities.

The IEC standard includes a procedure to analyze the influence of overspeeding based on tilt angular response and rotor torque characteristics measured in the wind tunnel, see chapter 6.

Wind turbine blades are often tested in low turbulent flows. The lack of turbulence in these simulations corresponds to full scale conditions due to the large relative wind velocities originating from the large angular velocity of the blade itself.

2.3 Keulegan-Carpenter number

The influence of the Keulegan-Carpenter number is described in several text books, see e.g. Sumer and Fredsøe 2006.

For a low turbulent flow with a wind velocity of v, the similarity of the forces acting on a rotating rotor depends on the Keulegan-Carpenter number KC defined as:

$$KC = \frac{v/n}{d} = \frac{(An+B)/n}{d} \approx \frac{A}{d} \tag{5}$$

in which n is the rotation frequency, d is a characteristic dimension, e.g. the diameter of the swept rotor area, and A and B are the slope and offset of the cup anemometer calibration equation corresponding to one puls per revolution. For a WindSensor cup anemometer the Keulegan-Carpenter number is equal to approx. 1.2/0.2 = approx. 6.

The magnitude of the Keulegan-Carpenter number is in a range where force coefficients for a single cup may depend on the actual Keulegan-Carpenter. If the cup anemometer is exposed to low turbulent flow, the Keulegan-Carpenter number will be a fixed number not depending on the wind velocity. However, if the cup anemometer is exposed to turbulent flow, the Keulegan-Carpenter number will change due to turbulence variations at frequencies above the cup anemometer rotation cut-off frequency.

The dependence on the Keulegan-Carpenter number may be crucial for rotor torque measurements in a wind tunnel. Fixing the rotation at another frequency than that corresponding to the wind tunnel velocity, as done in the Accuwind project, will fix the Keulegan-Carpenter number to a constant value not experienced in actual full-scale turbulence. Thus, step response measurements may give more accurate results measuring rotor torque characteristics due to a better representation of the varying Keulegan-Carpenter number in turbulent flow.

The step response procedure recommended here has been applied in the measurements of rotor torque characteristics described in section 6.2.

It is not possible on the present basis to quantify accurately the influence of the Keulegan-Carpenter number.

3. WIND TUNNEL AERODYNAMICS

The basic principles of open and closed wind tunnels are outlined in section 3.1 below. Section 3.2 describes the influence of blockage and selected calibration results showing interference effects between tunnel boundaries and rotating rotors are outlined in section 3.3.

3.1 Wind tunnel setups

The flow simulated and the pressures and suction generated at the cup anemometer including the mounting system are shown below in figure 5 for open and closed wind tunnels, respectively.

A CFD simulation was carried out using a simple box model wind tunnel geometry with a rotating disc to mimic the rotor. Dimensions for the wind tunnel and the anemometer were chosen to mimic typical dimensions in calibration tunnels. The mean wind velocity was 10 m/s, and the angular velocity of the disc was 8.3 rotations/s. Preliminary results are presented in figure 5, which shows a snapshot of the boundary layer pressure distribution. The pressure was calculated two millimeters below the wind tunnel ceiling along the wind tunnel center line. Following a minor increase in the pressure in front of the anemometer, we observe a significant decrease in the pressure above the anemometer. This result suggests a non-negligible interaction between the anemometer and the surrounding walls in the wind tunnel.

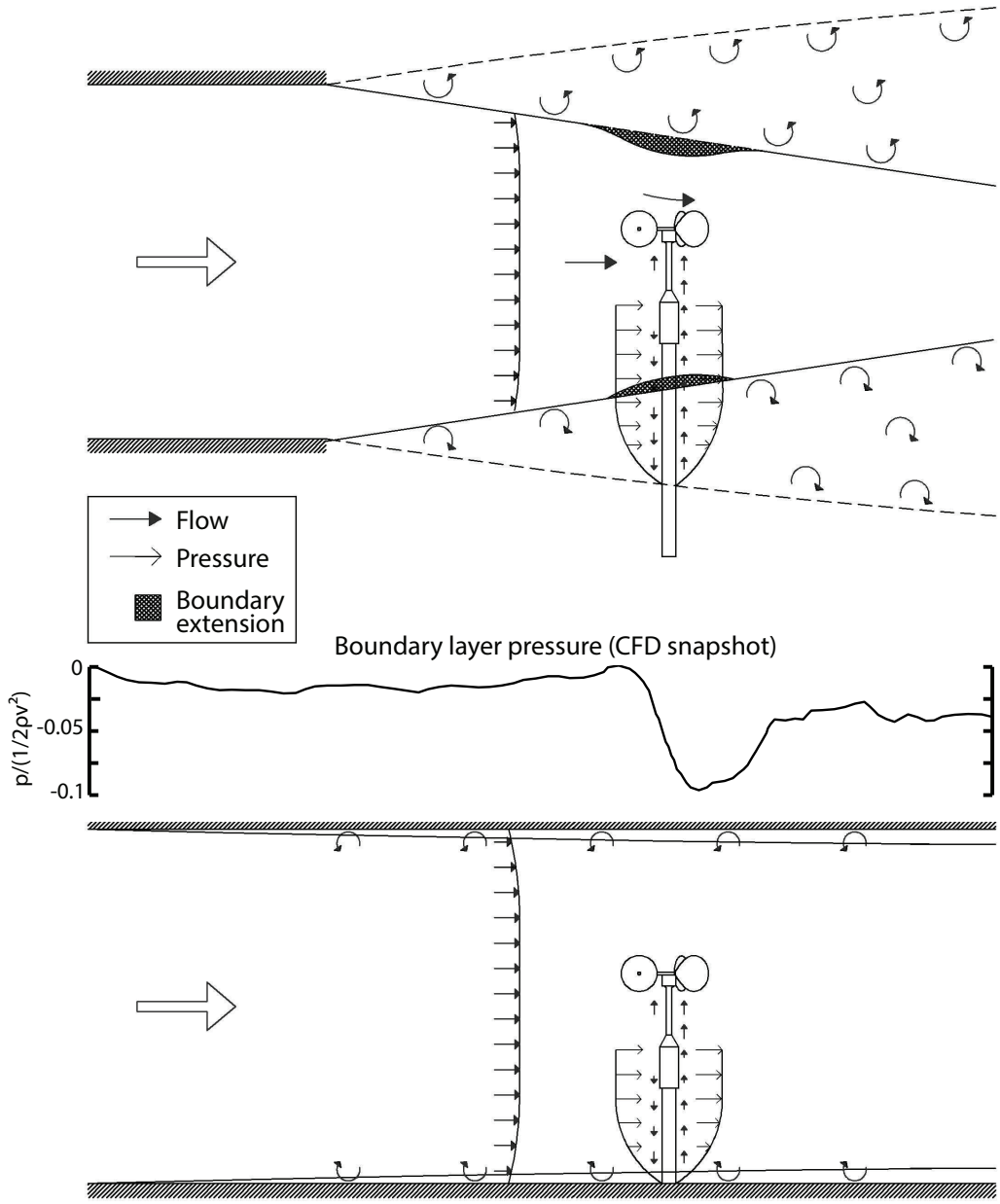

Figure 5. Principal sketch of the flow in open wind tunnels (above) and closed wind tunnels (below). The effective cross section due to boundary conditions is shown. Expected wind flow and pressure forces are indicated by arrows (see legend). The pressures on the front side of the mounting system and the suctions on the back side depend on the distances from the tunnel boundary and the rotor, see the illustration above. These non-constant pressures and suctions generate vertical flows as illustrated in the figure, and these flows influence the calibration equation, i.e. the conversion between incoming wind velocity and rotor rate.

For the open tunnel shown in the upper part of figure 5, an increased air entrainment from the surroundings, due to a local pressure decrease around the anemometer, is expected.

3.2 Influence of Blockage

Maskels blockage correction factor has been used extensively in many wind tunnels during many years. Maskell has shown that blockage results in two distinct phenomena: a drag increment due to wake distortion and a change in dynamic pressure. Wake distortion gives for the present blockage ratios a correction of the wind velocity of less than approx. 0.1%. The change in dynamic pressure may be expressed as a changed wind velocity v_b given by:

$$\frac{v_b}{v} = 1 + \frac{1}{2} a c_f b \tag{6}$$

where v is the wind velocity if blockage was not present, a is a factor depending on the shape of the structure in the wind tunnel, c_f is the force coefficient of the structure and b is the blockage ratio.

The blockage in the wind tunnel depends on the actual anemometers being calibrated. The focus here is on a closed wind tunnel with a cross-sectional area equivalent to a rectangle of 1.75 m x 1.2 m = 2.10 m². In this cross section a series of blockage investigations have been carried out. For all investigations described below the reference pitot tube is located upstream of the cross section with one or two cup anemometers, and the anemometers do not influence the wind at the pitot tube significantly. Furthermore, the cup anemometer rotors are in all the tests 60 cm above the tunnel floor indicating that the boundary effects covered in section 3.3 below are of the same magnitude for all calibrations carried out.

The rotor area is determined as the projected area perpendicular to the wind direction of the area swept by the rotor. The area of a cup anemometer and the mounting tube typically has a magnitude of 0.020 m² – 0.025 m². This gives a blockage ratio of approx. 1% - 2% for one cup anemometer present in the wind tunnel and 2% - 4% for two cup anemometers, see table 1. This is in accordance with the IEC requirement of a maximum blockage ratio of 5%.

Table 1. Blockage ratios for Windsensor and Thies cup anemometers.

Anemometer type	Windsensor		Thies	
Number of cup anemometers in the tunnel	1	2	1	2
Anemometer area [m^2]	0.018	0.035	0.024	0.049
Mounting tube area [m^2]	0.009	0.018	0.011	0.022
Total blockage area [m^2]	0.027	0.053	0.037	0.073
Blockage ratio, b [%]	1.263	2.527	1.745	3.491

The factors of a and c_f are determined by calibrations carried out in the different test setups, see table 2. The last column shows the velocity increases.

It is important to note that the blockage correction factors are determined for the present wind tunnel cross section geometry and they should be used with caution for other wind tunnel setups.

Table 2. Measured shape and force coefficient. The Thies cup is a Thies First Class.

Calibrated anemometer	Anemometer placed in the other side of the wind tunnel	$a \cdot c_f$	$\frac{v_b}{v}$
Windsensor	Windsensor (fixed rotor)	1.13	1.014
	Windsensor (rotating rotor)	0.78	1.010
	Thies (rotating rotor)	0.94	1.014
Thies	Thies (fixed rotor)	1.27	1.022
	Thies (rotating rotor)	1.17	1.020
	Windsensor (rotating rotor)	1.07	1.016

The following is observed from table 2:

- For Windsensor the $a \cdot c_f$ factor is approx. 0.8-0.9 when the cup anemometer in the other side of the wind tunnel is rotating.
- For Thies the $a \cdot c_f$ factor is approx. 1.1-1.2 when the cup anemometer in the other side of the wind tunnel is rotating.
- The $a \cdot c_f$ factor is increased slightly when the rotor is fixed in the other side of the tunnel. Thus, the blockage taken into account should reflect that the rotors are rotating.
- The Thies cup anemometer is more sensitive to blockage indicated by its larger $a \cdot c_f$ factor.

It is promising to observe the almost identical $a \cdot c_f$ factors for the setups with a Windsensor and a Thies cup anemometer in the wind tunnel at the same time, i.e. the correction factor does not depend on the actual cup anemometer calibrated.

Other investigations have been claimed to show that the Maskel blockage correction is not valid for cup anemometers, see Westermann et al 2011 and Gray 2007. These investigations assume that wind velocity ratios are equal to cup anemometer frequency ratios. Thus, the cup anemometer offset and the change of its slope due to blockage are not taken into account, and this gives very deviating results.

An example based on calibrations carried out in 2 Measnet approved wind tunnel cross sections: A WindSensor cup anemometer has a calibration equation of v=0.612n+0.199 and v=0.622n+0.178 in a small and large wind tunnel cross section, respectively, without any blockage correction applied. Inserting a pulse frequency n of 16 Hz gives the wind velocities of 9.99 m/s and 10.13 m/s, respectively. Thus, the same frequency gives 1.4% deviation in wind velocity showing that the IEC proposed blockage corrections based on frequency ratios are not representative for the relevant wind velocity ratios and should be deleted.

In conclusion, Maskel's blockage correction factor is found to be in reasonable agreement with the measurements presented and is therefore recommended.

3.3 Calibration results

The wind tunnel area of the open wind tunnel considered is $196 \cdot 10^4$ mm^2, which is the quadratic cross section of the outlet nozzle with height = width = 1400 mm. However, the effectual cross-section of the tunnel is due to boundary conditions estimated to be approx.

1000 x 1000 mm. The transition from laminar to turbulent flow has been validated by the use of a low density twine flag which responds easily to the wind.

The heights of the two closed tunnels are 0.85 m and 1.2 m, respectively, and their width is 1.75 m. The boundary layers of the two closed tunnels have a thickness of approx. 50 mm.

In figure 6 below, the reference distance to floor in both of the closed wind tunnels is equal to 600 mm, and in the open wind tunnel it is 800 mm from the outlet bottom level. All three wind tunnels have a homogeneous flow field in the heights tested of ±50, ±100 and ±150 mm from the reference position. Thus, the changes in calibration results originate from changes in blockage ratios and tunnel boundary interference effects.

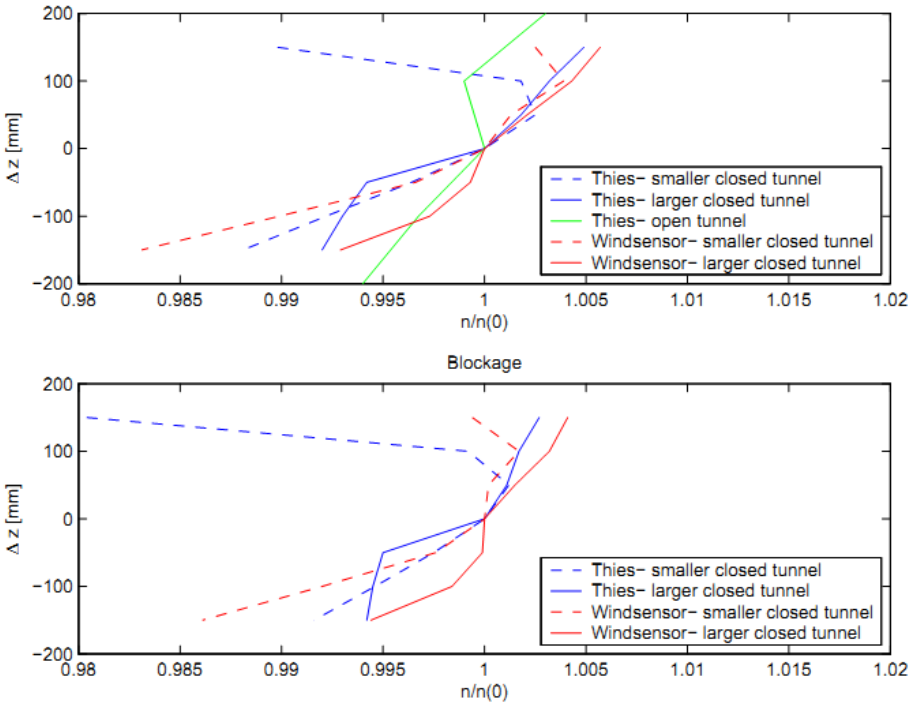

Figure 6. Standard calibration results measured in an open and two closed wind tunnels. The Measnet calibration carried out in each point have been converted to a frequency corresponding to 10 m/s, and the x-axis show the frequency ratios between calibrations carried out as function of vertical distance to the wind tunnel reference position. No blockage correction in the top figure, blockage correction in accordance with section 3.2 in the figure below.

Figure 6 shows that:

- The calibration results depend on the vertical location in all three wind tunnels.
- For the larger closed tunnel the frequencies increase with height for all locations tested.
- When the cup anemometer is moved down to smaller distances to floor, the decrease in frequency is up to approx. 1.5% and approx. 1% for the WindSensor and Thies anemometer, respectively.
- When the cup anemometer is moved up to smaller distance to the ceiling the smaller wind tunnel with a height of 0.85 m shows reduced frequencies due to the friction at the roof.

For the height of 1.2 m, the frequencies are increasing when the cup anemometer location is moved up, and this indicate that the friction at the roof now is reduced due to the larger roof distances of 450 mm or more.

- Blockage correction in the open tunnel will move the curve further away from a vertical position, if introduced.

The observations above show that the floor influences the calibration results for all heights tested of 450 to 750 mm from the floor. Furthermore, the friction at the roof slow down the rotor for distances to the roof of below approx. 500 mm, and the influence increases with decreasing distance to the roof. For the smaller wind tunnel the two effects merge together and are difficult to separate from each other.

The flow around circular cylinders depends on their slenderness defined by its length divided by their diameter. For the closed wind tunnels, the slenderness of the mounting may be judged by the distance from rotor to tunnel floor divided by tube diameter disregarding that the anemometer shaft has other diameters. In the reference position the slenderness become 600/25=24 and 600/35=17.1 for the WindSensor and Thies cup anemometer, respectively. Results for circular cylinders show that the flow around the structure starts to become 3-dimensional for a slenderness of less than approx. 100. Thus, the 3-dimensional effects around the mounting system are one aspect of a full understanding of the results presented in figure 6.

4. MEASNET/IEC STANDARD CALIBRATION PROCEDURE

Cup anemometers have been calibrated extensively by many wind tunnels over the last approx. two decades. In order to standardize and improve the calibrations carried out Measnet prepared their calibration procedure published in 1997 and has arranged regularly inter comparisons, so-called round robins, between Measnet members in anemometer calibrations. The first Measnet inter comparisons organized in 1994 gave calibration deviations of up to approx. 10% of measured wind speed between the wind tunnels. This band has been narrowed down substantially with deviations of the order of 1% in the most recent inter comparisons carried out.

The original Measnet calibration procedure was incorporated as an Annex into the 2005 edition if IEC 61400-12-1 international standard. The IEC procedure, especially its requirements to flow characteristics and wind tunnel size including tunnel boundary effects, is expected to be changed in the revised IEC standard expected to be completed in 2013.

The present Measnet/IEC standard calibration procedure is described in Measnet: “Anemometer calibration procedure”, version 2, October 2009. The procedure is based on the specifications given in 61400-12-1:2005: Wind turbines – Part 12-1: Power performance measurements of electricity producing wind turbines”, First edition 2005-12 / Annex F: “Cup anemometer calibration procedure”.

The Measnet calibrations should be performed under both rising and falling wind speed in the range of 4 m/s to 16 m/s at a calibration interval of 1 m/s or less. The wind velocity range specified facilitates that the calibration covers crucial wind velocities for power performance of wind turbines. A larger calibration range, e.g. to larger wind velocities, would have given less accuracy in the most crucial wind velocity range for wind turbines.

The following wind tunnel requirements are included as part of the procedure:

1. The blockage ratio – defined as the ratio of the anemometer frontal area including its mounting system to the total test section area should not exceed 10% for an open test section and 5% for a closed test section.
2. The flow across the area covered by the anemometer should be uniform to 0.2%.
3. The axial turbulence intensity at the anemometer's position should be below 2%.
4. The anemometer should be positioned at the test section perpendicular to the flow field of the wind tunnel as accurate as possible. The maximum deviation allowed is 1°.

The wind tunnel facility should prove through round robin testing that its results are comparable with other anemometer calibration facilities. The wind velocity deviation from the round robin Measnet average should be within 1%.

The tunnel factor is determined as ratio of pitot-tube measurements. The interference effects between tunnel boundaries and the rotating cups are not included specifically in the procedure, and this turns out to be a crucial parameter for small wind tunnels.

5. STANDARD CALIBRATION RESULTS

The Measnet standard calibration procedure enables the results described below. Repeatability and bias are focused on in section 5.1 to 5.2, respectively.

5.1 Repeatability

The present status of cup anemometer calibrations is that each wind tunnel may have an extremely good repeatability. Figure 7 shows the distribution of the calibration results obtained for 1000 different WindSensor P2546A-OPR with rotors molded in one piece. It is seen that their coefficient of variation of the calibrated wind speeds at 10 m/s is approx. 0.1%.

The distribution of the calibration results obtained for other precision cup anemometers have a variability of approx. 3 to 5 times the variability of WindSensor P2546-OPR. These distributions are also illustrated in figure 7.

The wind tunnel variability in the same period is shown in figure 8 by the distribution of calibration results for the same WindSensor cup anemometer. Typical variations due to the wind tunnel are seen to be less than 0.05%, and the largest variations are below ±0.2%. It is observed that the wind tunnel contribution to the variability of the precision cup anemometers is insignificant, even for the WindSensor P2546A-OPR with extremely small variability.

It may be concluded from figures 7 and 8 that the use of WindSensor P2546A-OPR cup anemometers calibrated by Svend Ole Hansen ApS reduces the risk of outliers to be much less than one to a million.

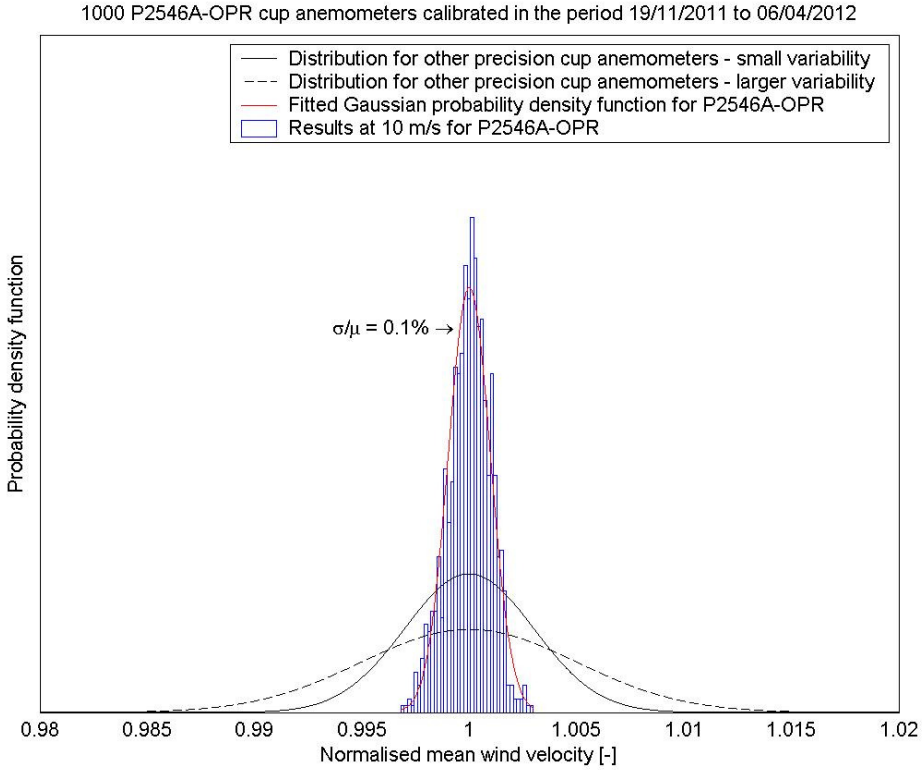

Figure 7. Distribution of calibration results for 1000 different WindSensor P2546-OPR.

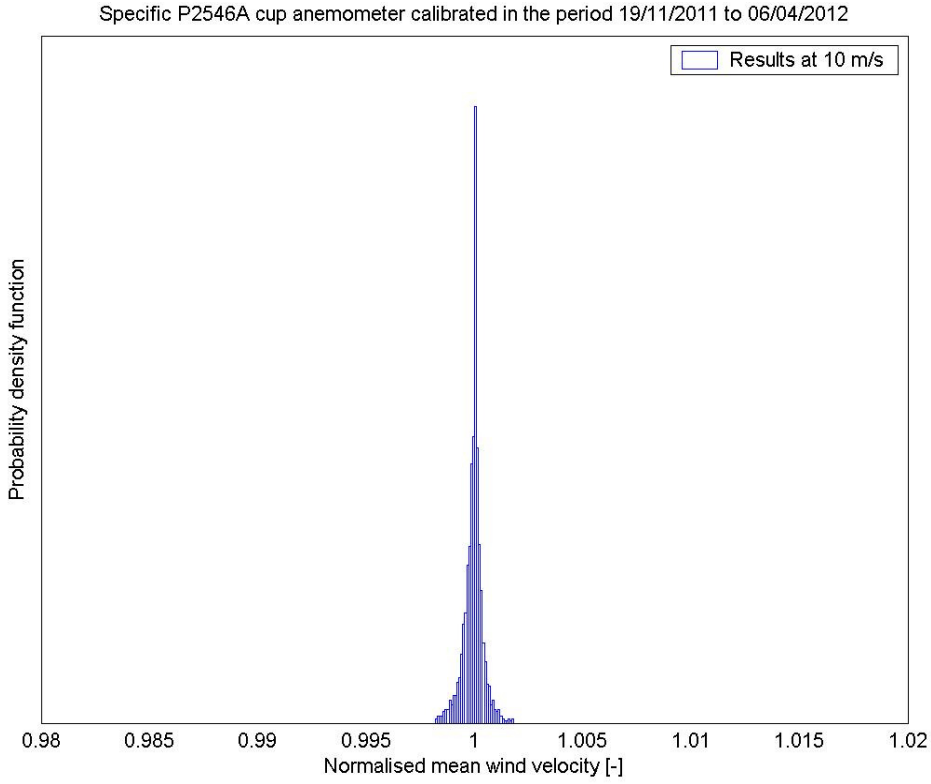

Figure 8. Distribution of calibration results for the same WindSensor P2546A

5.2 Bias from wind tunnel to wind tunnel

In spite of the good repeatability as shown above for a single wind tunnel, different wind tunnels may still have wind speed differences of up to typically 1% between their calibration results obtained for the same cup anemometer, and the differences may depend on the cup anemometer type calibrated. A possible outcome of this is illustrated in figure 9.

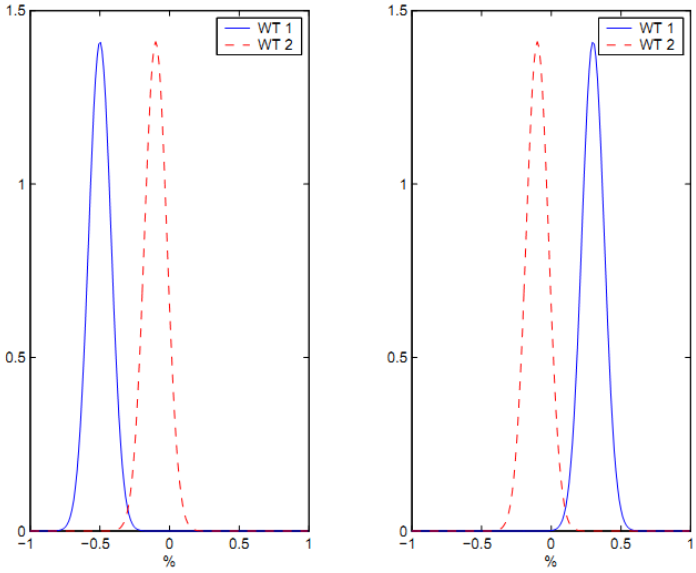

Figure 9. Bias between wind tunnels described by distributions

The main reason for the systematic bias between wind tunnels may be the influence of blockage and the interference between rotating cup anemometer rotors and tunnel boundaries. The typical Measnet wind tunnel is approx. 1 x 1 m in dimension, and this has turned out to be too small for avoiding the blockage and tunnel boundary interference effects that may give biased calibrations using the present procedures.

There is a profound need of reference calibrations of different cup anemometers carried out in large wind tunnels with cross sectional areas of approx. 5-10 m², where the effect of blockage and tunnel boundary interference are negligible. The calibration uncertainty in the large wind tunnels may be as low as approx. 0.1% indicating that the calibration results will be almost without any systematic bias.

Calibrations of different reference cup anemometers in several wind tunnels of varying type and cross sectional areas from approx. 1 m² to 10 m² will facilitate an accurate estimation of blockage and tunnel boundary interference effects, and correction factors may enable the small wind tunnels to carry out accurate calibrations without large systematic bias introduced by blockage and tunnel boundary interference effects.

6. CLASSIFICATION OF CUP ANEMOMETER

Tilt response and torque measurements are described in section 6.1 and 6.2, respectively.

6.1 Tilt angular measurements

Figures 10-12 shows typical results of tilt response measurements for anemometers. The tilt angular responses are determined by carrying out standard calibrations for different selected

tilt angles, where the cup rotor position in the wind tunnel is fixed at the location for standard calibrations. The other end of the mounting tube is fixed to a machine formed as an arch, which enables that the cup anemometer rotor plane is only rotating around a horizontal axis perpendicular to the wind direction, i.e. no horizontal or vertical movements of the cup rotor. The machinery is below the tunnel floor, and the tube passes sealed through the tunnel floor.

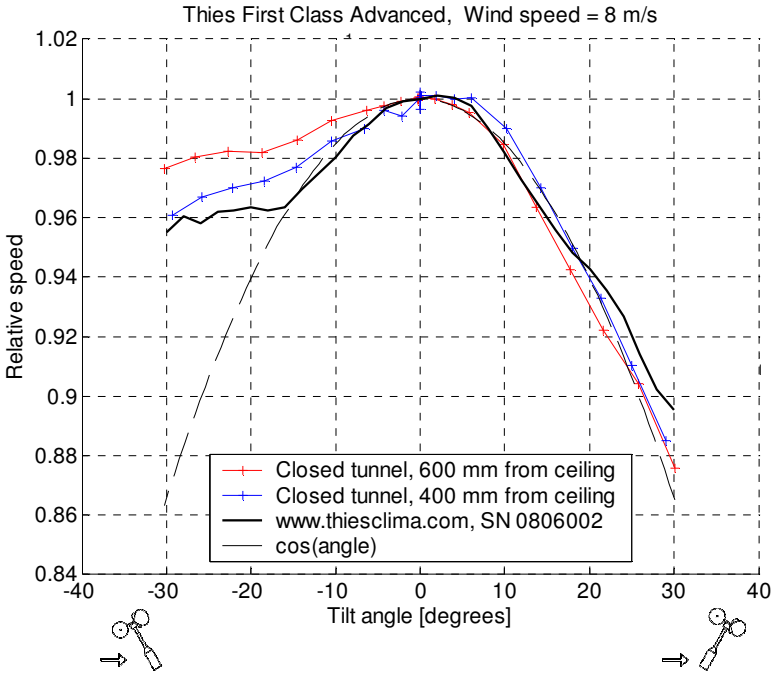

Figure 10. Tilt angular response measurements and their dependence on tunnel height

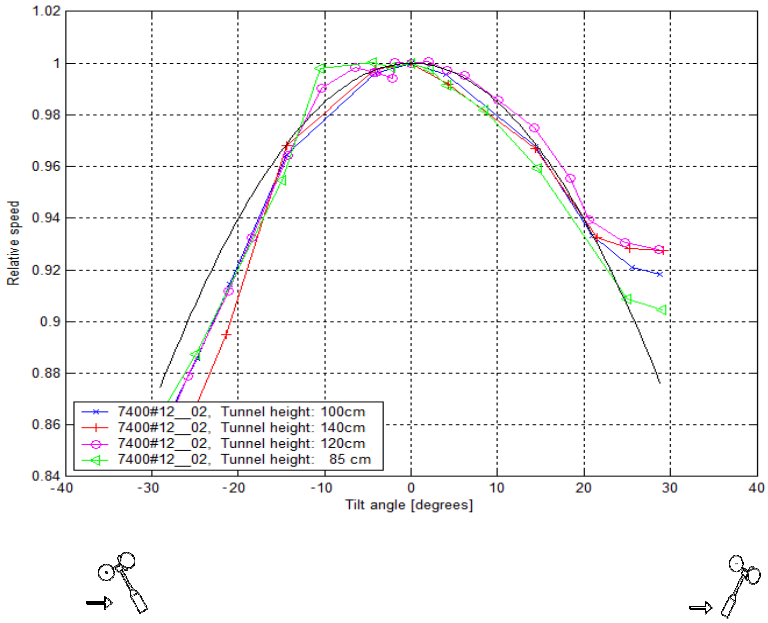

Figure 11. Tilt angular response measurements and their dependence on tunnel height

Figures 10 shows that the tilt angular responses measured for Thies First Class Advanced anemometers may be influenced by the tunnel ceiling if the distance between rotor and ceiling is less than 600 mm. The same observation is made for the tilt angular response measured for another cup anemometer illustrated in figure 11. Since the measuring height is

600 mm above the floor, it may be concluded that accurate measurements require a tunnel height of at least 1.2 m.

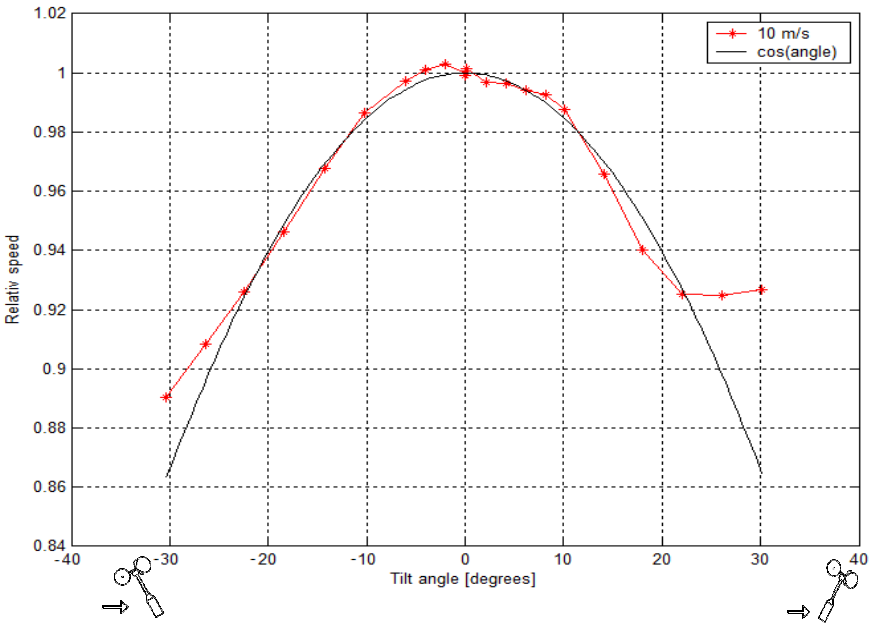

Figure 12. Tilt angular response of a prototype of a new WindSensor cup anemometer

The tilt angular response shown in figure 12 for a prototype of a new WindSensor cup anemometer shows a very good match to the target cosine dependence. The deviation from target is only significant for angles above approx. 25 degrees

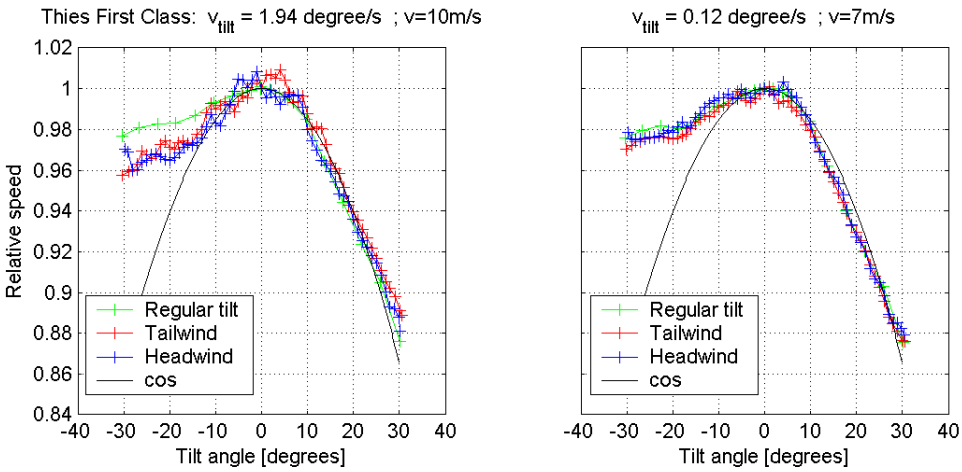

Figure 13. Tilt angular calibration results for a rotating setup at low angular velocity (right plot) and high angular velocity (left plots). Illustration of the Coriolis effect and its dependence of tailwind (red curve) and headwind (blue curve) in relation to regular stationary tilt (green curve).

In sweeps the mounting system is rotated around a horizontal axis through the rotor plane with an angular velocity designated v_{tilt} in figure 13 above. Sweeps are allowed in the IEC standard and the Accuwind results were based on sweeps with a rate of approx. 2 degree per

second. For sweeps with an angular velocity of approx. 2 degree per second, as shown above in figure 13, the Coriolis accelerations introduced by the sweep and the cup velocity influence the tilt angular response significantly for both head wind and tail winds. Slower sweep rates reduce the effect, see right-hand figure 13.

Methods for classification of cup anemometers were developed in the European research project Accuwind, and the methods were subsequently implemented in the IEC 61400-12-1 standard on power performance measurements. The Accuwind results have been based on measurements carried out in an open and closed wind tunnel with cross sections having heights x widths of 0.8 x 1.0 m and 0.675 x 0.9 m, respectively. The tilt angular response measurements were informed to be carried out using sweeps with a rate of approx. 2 degree per second. The results presented in figures 10-11 and 13 documents that the limited tunnel heights of 0.8 and 0.675 m, respectively, and the sweep rate used in Accuwind project will give systematic bias of the tilt angular responses determined in Accuwind.

It is recommended that the revised IEC standard specifies minimum sizes of wind tunnel cross sections for tilt angular response measurements and recommends to measure at fixed tilt angles, i.e. without any sweep during the measurements. This is the only way of assuring that the systematic bias from tunnel boundary interference effects and from the Coriolis effect will not influence the tilt response measured independently of cup anemometer type.

6.2 Rotor torque measurements

The physical parameters of the mathematical model of section 2.1 can be determined experimentally. The angular velocity of a cup anemometer in a steady wind is forced off of its equilibrium rotation via an internal mechanism. The motion is captured with a high-speed camera and the angular position and velocity is computed. By comparison to the mathematical model the physical parameters C can be determined and the off-equilibrium torque subsequently determined.

Figure 14 shows a typical time history measured by the high-speed camera, and figure 15 shows the torque characteristics of a cup anemometer. The angular velocity illustrated in figure 14 is measured in a flow with a turbulence intensity of approx. 1% indicating that fluctuations are generated also by the cup anemometer itself.

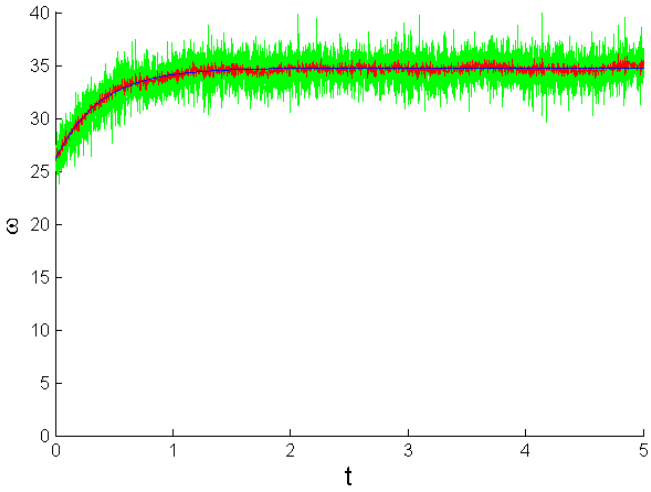

Figure 14. Typical time history of angular velocities (green) of 10 repetitions of an experiment at $v = 7$ m/s where the anemometer rotation is slowed and released. The mathematical model (blue) is fitted to the ensemble average (red) of the repetitions.

The developed procedure described above differs from previous used methods established in the Accuwind project. The procedure developed is judged to give a better representation of the full-scale cup anemometer behavior due to the more accurate simulation of the Keulegan-Carpenter number described in section 2.3.

It should also be emphasized that the cup anemometer geometry is not changed in the tests carried out. The high-speed camera facilitates that the number of pulses per revolution is not crucial for obtaining a sufficient resolution of the transient time history measured. The resolution obtained is found to be better than possible resolutions for the commercial cup anemometers having most pulses per revolution.

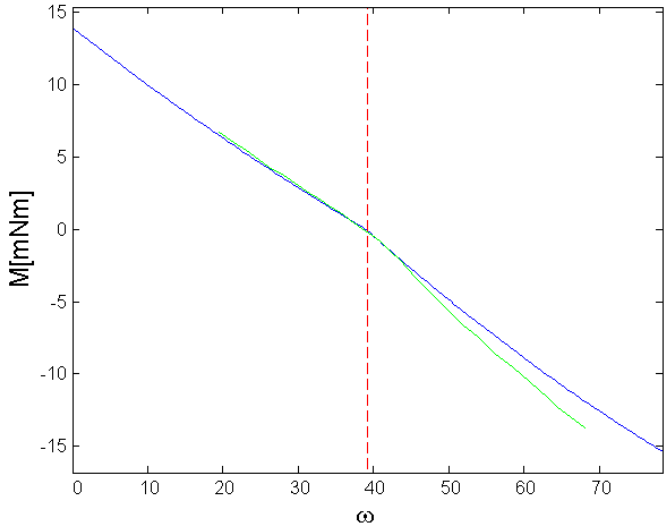

Figure 15. Torque curves (blue) of an anemometer as a function of angular velocity ω for a v=8 m/s wind speed. The equilibrium angular velocities are marked by the dashed red lines. The green torque curve from the IEC 61400 code is shown as reference. The IEC curves based on torque measuremnts at fixed rotations and may be influenced by non-scaled Keulegan-Carpenter numbers.

7. CONCLUSION

The cup anemometer aerodynamics outlined in the paper specify the differential equation describing the motion of the cup rotor and subsequently focus on the influence of turbulence of the incoming air and non-similarities of the Keulegan-Carpenter number in rotor torque measurements with forced cup rotor rotations at fixed rates. It is not possible on the present basis to quantify accurately the influence of air turbulence and the Keulegan-Carpenter number. However, in order to avoid a possible systematic bias, calibrations in simulated air turbulence and with a correct Keulegan-Carpenter number must be preferred. The paper includes a proposal for simulation of air turbulence focussing on the importance of small-scale turbulence.

The paper documents that systematic bias may be introduced using some of the IEC procedures and it is recommended that the new findings of the present paper are taken into account in the ongoing revision of the IEC standard.

Some of the uncertainties presently encumbered in the calibrations carried out may originate from the size of the Measnet approved wind tunnels. It is shown that a minimum distance from rotor to tunnel boundary is crucial for not having interference effects between the tunnel boundary and the rotating rotor. If this distance is too small the tunnel boundary is sucked towards the rotor in open tunnels or a friction force is generated in closed tunnels. The interference effects may influence the calibration carried out significantly for small wind tunnels.

The IEC procedure and the Round Robins organized by Measnet have reduced the calibration wind speed deviations from tunnel to tunnel down to approx. 1%. It is not likely that this deviation range can be reduced much further without revising the calibration procedure details.

In the future calibration procedure two objectives are important:

1. The calibration results should reflect the true wind without any significant bias.
2. The deviations from tunnel to tunnel should be reduced from the Measnet allowable limit ±1% to a limit of the order of ±0.25 to ±0.5%.

Both objectives may be obtained by carrying out reference calibrations in large wind tunnels and use these results to estimate the actual true wind measured by selected anemometers, i.e. objective no. 1 is met. Tunnel correction factors to be used in small wind tunnels should be determined by calibrating the same anemometers in these tunnels. Thus, the procedure described facilitates that both objectives nos. 1 and 2 above are met.

The results obtained in the large wind tunnels will give basis for understanding the interference effects in detail and to quantify their importance in different wind tunnel setups.

ACKNOWLEDGEMENTS

The many constructive comments received from the experts of the Measnet anemometer group are highly acknowledged.

REFERENCES

1. Kristensen, L., Hansen, O.F. and S.O. Hansen: “Addendum to: Bias on horizontal mean-wind speed and variance caused by turbulence”, www.windsensor.dk, May 29, 2012.
2. Kristensen, L. and O.F. Hansen: “Bias on horizontal mean-wind speed and variance caused by turbulence”, www.windsensor.dk, May 27, 2012.
3. Westermann, D; N.Balaresque and P. Busche: “Systematic deviation in anemometer calibration due to geometrical interference”, Deutsche WindGuard, 2011.
4. Gray, N.M.B.: Effecto obstructive o “blockage” en la calibracion de anemometros”, Deutsche WindGuard, Universidad Tecnica Frederico Santa Maria and Tuhn, 2007.
5. Dahlberg, J.-Å, Pedersen, T.F. and P. Busche: “ACCUWIND – Methods for classification of cup anemometers”, Risø National Laboratory, Risø-R-1555 (EN), May 2006.
6. Sumer, M.S. and J. Fredsøe: “Hydrodynamics around cylindrical structures”, World Scientific, 2006.
7. Kristensen, L.: “Cup anemometer behavior in turbulent environments”, Journal of Atmospheric and Oceanic Technology, Volume 15, page 5-17, February 1998.

8. Dyrbye, C. and S.O. Hansen: “Wind loads on structures”, John Wiley & Sons, 1997.
9. Kristensen, L.: “The cup anemometer and other exciting instruments”, Risø National Laboratory, Roskilde, Denmark, April 1992.
10. Jensen, M: and N. Franck: “Model-scale tests in turbulent wind”, The Danish Technical Press, Copenhagen, 1965.